Monthly Notices
of the
ROYAL ASTRONOMICAL SOCIETY

Mon. Not. R. Astron. Soc. **427,** 1252–1265 (2012) doi:10.1111/j.1365-2966.2012.22059.x

Plunging fireworks: why do infalling galaxies light up on the outskirts of clusters?

Smriti Mahajan,[1,2]★ Somak Raychaudhury[1] and Kevin A. Pimbblet[3,4]

[1] *University of Birmingham, School of Physics and Astronomy, Birmingham B15 2TT*
[2] *University of Queensland, School of Mathematics and Physics, Brisbane, QLD 4072, Australia*
[3] *Monash Centre for Astrophysics, Monash University, Clayton, VIC 3800, Australia*
[4] *School of Physics, Monash University, Clayton, Melbourne, VIC 3800, Australia*

Accepted 2012 September 4. Received 2012 September 2; in original form 2012 May 9

ABSTRACT

Integrated star formation rate (SFR) and specific star formation rate (SFR/M^*), derived from the spectroscopic data obtained by the Sloan Digital Sky Survey (SDSS) data release 4 (DR4), are used to show that the star formation activity in galaxies ($M_r \leq -20.5$) found on the outskirts (1–$2r_{200}$) of some nearby clusters ($0.02 \leq z \leq 0.15$) is enhanced. By comparing the mean SFR of galaxies in a sample of clusters with at least one starburst galaxy (log SFR/$M^* \geq -10\,\mathrm{yr}^{-1}$ *and* SFR $\geq 10\,\mathrm{M}_\odot\,\mathrm{yr}^{-1}$) to a sample of clusters without such galaxies ('comparison' clusters), we find that despite the expected decline in the mean SFR of galaxies towards the cluster core, the SFR profile of the two samples is different. Compared to the clusters with at least one starburst galaxy on their outskirts, the galaxies in the 'comparison' clusters show a lower mean SFR at all radius ($\leq 3r_{200}$) from the cluster centre. Such an increase in the SFR of galaxies is more likely to be seen in dynamically unrelaxed ($\sigma_\mathrm{v} \gtrsim 500\,\mathrm{km\,s}^{-1}$) clusters. It is also evident that these unrelaxed clusters are currently being assembled via galaxies falling in through straight filaments, resulting in high velocity dispersions. On the other hand, 'comparison' clusters are more likely to be fed by relatively low density filaments. We find that the starburst galaxies on the periphery of clusters are in an environment of higher local density than other cluster galaxies at similar radial distances from the cluster centre. We conclude that a relatively high galaxy density in the infalling regions of clusters promotes interactions amongst galaxies, leading to momentary bursts of star formation. Such interactions play a crucial role in exhausting the fuel for star formation in a galaxy, before it is expelled due to the environmental processes that are operational in the dense interiors of the cluster.

Key words: galaxies: clusters: general – galaxies: evolution – galaxies: starburst – cosmology: observations – large-scale structure of Universe.

1 INTRODUCTION

Statistical analyses of large samples of galaxies belonging to rich galaxy clusters reveal a gradual trend of the quenching of star formation in galaxies at decreasing radial distance from the centres of clusters. This is generally interpreted as the overwhelming influence of the gravitational field of the dark matter associated with the cluster, added to the effect of the hot gas in the intracluster medium (ICM), that serves to progressively deprive the galaxies of the fuel for star formation through tidal and other stripping processes. Thus, the core of a cluster is generally thought to be the site of the most dramatic transformation in the evolution of a galaxy. As a result, the central regions of galaxy clusters end up being dominated by passively evolving red elliptical/lenticular galaxies, while their blue star-forming counterparts prefer the sparsely occupied regions away from clusters.

However, over the last few years, a growing number of galaxies, with an unusually high rate of star formation, have been discovered on the outskirts of rich galaxy clusters. These galaxies, often spotted close to or outside the virial radius of clusters, are seen to possess tidal features, and signs of morphological distortions that appear to be induced by close interactions. A majority of these galaxies have been discovered beyond a redshift of $z = 0.2$ (Keel 2005; Moran et al. 2005; Sato & Martin 2006; Marcillac et al. 2007; Oemler et al. 2009), since at these redshifts, the

★E-mail: s.mahajan1@uq.edu.au

regions beyond the virial boundaries of clusters often fit on to current wide-format imagers. Good examples of these are the infalling galaxy C153 in Abell 2125 ($z = 0.246$; Wang, Owen & Ledlow 2004), which exhibits comet-like tails of X-ray emitting gas, or the flagrantly star-forming galaxies on the outskirts of Abell 2744 ($z = 0.4$; Braglia, Pierini & Böhringer 2007), which seem to lie on filaments feeding a set of merging clusters, and in the lensing cluster CL0024+16 ($z = 0.4$; Moran et al. 2005), where enhanced star formation is detected in a string of early-type dwarfs outside the virial radius.

It is not yet known whether such galaxies are common at lower redshifts, since surveys away from the cores of nearby clusters are not common. Infalling galaxies like NGC 4472, at 1.2 Mpc from the core of the Virgo cluster ($z = 0.003$), show evidence of extended streams of hot X-ray emitting gas, and a shock front in the X-ray observation (Kraft et al. 2011). This is accompanied by star formation in tidal streams of stripped cold gas from its dwarf companion UGC 7636 (Lee, Richer & McCall 2000). Similar systems are seen elsewhere in Virgo (Abramson et al. 2011), and in Abell 3627 ($z = 0.016$; Sun et al. 2010), where the abundance of Hα and H II emission indicate rapid star formation. Some of these galaxies are plunging towards the cluster core on their own, while others like those comprising J0454 ($z = 0.26$) are merging with the cluster as a galaxy group (Schirmer et al. 2010). In the absence of systematic studies, it is not clear how common such starburst galaxies are away from the cores of clusters, and indeed how important this phenomenon is in the grand scheme of galaxy evolution. One would like to know, for instance, whether their occurrence is related to the properties of the clusters, the structure of the surrounding cosmic web or the properties of the galaxies themselves.

Earlier studies have suggested that evolution of galaxies in clusters is mainly driven by processes such as ram-pressure stripping, where a galaxy falling into cluster loses its gas content through interactions with the hot ICM, thus being deprived of star formation by the time it reaches the cluster core. Major mergers between galaxies are uncommon even in cluster cores (De Lucia & Blaizot 2007), and galaxy–galaxy interactions (Moore et al. 1996) are in general thought to be unimportant in cosmological models (e.g. Mayer et al. 2006). However, the observed radial gradient in star formation and other galaxy properties (e.g. Boselli & Gavazzi 2006; Porter et al. 2008; Mahajan, Haines & Raychaudhury 2010), and the existence of transitional (i.e. post-starburst) galaxy populations to much farther distances from the centres of clusters than their region of influence (e.g. Gavazzi et al. 2010; Mahajan, Haines & Raychaudhury 2011a), indicate that the influence of the cluster does not tell the whole story.

In particular, repeated high velocity encounters between galaxies, often termed as 'harassment' (Moore et al. 1996), can play a special role in the evolution of galaxies in low- and intermediate-density environments (Lewis et al. 2002; Haines et al. 2006; Moss 2006; Porter & Raychaudhury 2007; Porter et al. 2008; Oemler et al. 2009; Smith et al. 2010, among others). The frequency and impact of such galaxy–galaxy interaction processes depend upon the local galaxy density. So, in principle, any location on the cosmic web, with galaxy density above a 'critical' value (see Gómez et al. 2003, for instance), should encourage interactions, resulting in bursts of star formation, among galaxies. It has been shown elsewhere that filaments of galaxies (Porter & Raychaudhury 2007; Boué et al. 2008; Fadda, Biviano & Durret 2008; Porter et al. 2008; Edwards, Fadda & Frayer 2010a; Biviano et al. 2011) and outskirts of clusters (Rines et al. 2005; Smith et al. 2010; Coppin et al. 2011; Verdugo et al. 2012) are such favourable sites.

While simulations suggest that stripped H I and X-ray emitting gas should be ubiquitous and detectable in the central regions of most clusters (e.g. Tonnesen & Bryan 2010; Yamagami & Fujita 2011), it is difficult to quantify systematic properties of galaxies residing on inter-cluster filaments on the cosmic web due to the small numbers involved on a single filament. However, by stacking a large number of filaments, in the two-degree Field Galaxy Redshift Survey (2dFGRS), it has been shown that the star formation in galaxies is enhanced 3–4 Mpc from the cores of the clusters, suggesting that occurrence of burst of star formation in infalling galaxies should be a common phenomenon (Porter & Raychaudhury 2007; Porter et al. 2008).

Since outside the virial boundaries of clusters, the density of the ICM is too low to influence the incoming galaxies, it was suggested in these studies that the enhancement in star formation is due to high speed encounters occurring amongst infalling galaxies on the outskirts of galaxy clusters. Multiple starburst galaxies have been seen in similar single systems associated with filaments, such as in Abell 1763 ($z = 0.23$; Fadda et al. 2008). Multi-wavelength studies of photometric properties of galaxies belonging to the Shapley supercluster ($z = 0.048$) revealed that the supercluster environment might be solely responsible for the evolution of faint ($\gtrsim M^* + 2$) galaxies (Haines et al. 2011).

This paper addresses the issue of enhancement in star formation activity in galaxies found in the infall regions of nearby galaxy clusters. The star formation activity is quantified using the integrated star formation rate (SFR) and specific star formation rate (SFR/M^*) of galaxies in a representative sample of local clusters, and emission-line ratios to separate out the emission dominated by the active galactic nuclei (AGN) from that of star formation. A catalogue of large-scale inter-cluster filaments of galaxies, sourced from the Sloan Digital Sky Survey (SDSS), is used to evaluate the impact of the position of a galaxy in the cosmic web on its star formation properties.

The outline of the paper is as follows: the data and sample properties are elaborated in the following section. The star formation properties of cluster galaxies are described in Section 3, briefly discussing the behaviour of galaxies falling in the cluster for the first time. The impact of the immediate and the large-scale structure (LSS) environment on the star formation properties of galaxies is discussed in Section 4, and the main results are summarized in Section 5. Throughout this work a cosmology with $\Omega_{\rm m} = 1$, $\Omega_\Lambda = 0$ and $h = 70\,{\rm km\,s^{-1}\,Mpc^{-1}}$ was adopted for calculating distances and absolute magnitudes. We note that in the redshift range chosen for this work ($0.02 \leq z \leq 0.15$), the results are insensitive to the choice of cosmology.

2 THE SAMPLE

We used the spectroscopic galaxy data provided by the SDSS DR4 (Adelman-McCarthy et al. 2006), which uses two fibre-fed double spectrographs, covering a wavelength range of 3800–9200 Å. The resolution $\lambda/\Delta\lambda$ varies between 1850 and 2200 in different bands. The galaxy magnitudes and the corresponding galactic extinction values in the *r* band were taken from the New York University Value added galaxy Catalogue (NYU-VAGC; Blanton et al. 2005). The *k*-corrections (to $z = 0.1$) provided by Yang et al. (2007) were used to correct for the effect of distance on the magnitude of galaxies. Only those galaxies with absolute magnitude $M_r \geq -20.5$ (SDSS magnitude limit at the median redshift of our sample $z = 0.1$) were considered.

2.1 Cluster membership

All Abell clusters (Abell, Corwin & Olowin 1989) in the redshift range $0.02 < z \leq 0.15$ were considered. In order to assign galaxies to clusters differential redshift slices were used, i.e. galaxies, within a projected radius $R = 6$ Mpc of the cluster centre at the redshift of the cluster, were included if they were found to be within a redshift slice of

$$\Delta z = \left\{ \begin{array}{ll} 3000 \text{ km s}^{-1} & \text{if } R \leq 1 \text{ Mpc} \\ 2100 \text{ km s}^{-1} & \text{if } 1 < R \leq 3 \text{ Mpc} \\ 1500 \text{ km s}^{-1} & \text{if } 3 < R \leq 6 \text{ Mpc} \end{array} \right\}. \quad (1)$$

This differential velocity slice approach helps in reducing interlopers without following a rigorous procedure for assigning cluster membership, and hence is well suited for a statistical study like this. Note that popular methods, such as the $3\sigma_v$ velocity dispersion cut, which is often employed to define galaxy membership of clusters, are not our preferred choice because of our need to include the outskirts of clusters.

2.2 Cluster parameters

Once the galaxy members of the clusters were found as described in Section 2.1, their velocity dispersion (σ_v) is determined using the bi-weight statistics (ROSTAT, Beers, Flynn & Gebhardt 1990). Then assuming cluster mass $M(r) \propto r$, r_{200} (the radius at which the mean interior over-density in a sphere of radius r is 200 times the critical density of the Universe) was calculated, using the relation given by Carlberg, Yee & Ellingson (1997),

$$r_{200} = \frac{\sqrt{3}}{10} \frac{\sigma}{H(z)}. \quad (2)$$

Any comparison clusters (described below) which were not fully covered in DR4 were excluded along with any clusters for which reliable velocity dispersion information was neither available nor obtainable from the given data.

The final sample consists of 107 Abell clusters (Abell et al. 1989) with $z < 0.15$ lying in those regions of the sky where SDSS DR4 has more than 70 per cent spectroscopic coverage.

2.3 Galaxy data

The galaxy data (SFR, specific star formation rate, SFR/M^*) used in this paper were sourced from the catalogue of Brinchmann et al. (2004, henceforth B04) which is based on SDSS DR4. The Bayesian technique employed by B04 for modelling various physical parameters including SFR and SFR/M^* is advantageous over using a single emission line such as Hα or [O II] as a star formation indicator because the integrated SFR is a synthesized representation of various line indices. This reduces the uncertainty inherent in using a single index by several orders of magnitude. The simultaneous use of different indices enables us to separate the galaxies with a significant AGN component from those with emission entirely due to star formation (see below). Using the entire spectrum also makes it possible to obtain an independent estimate of the stellar mass M^* (from the z-band photometry), which further constraints the estimated SFR/M^*, making it a more reliable parameter for evaluating star formation properties of galaxies, relative to comparable luminosity-based parameters used elsewhere (e.g. Lewis et al. 2002).

B04 divided all galaxies into star forming, AGN and composite using the BPT (Baldwin, Phillips & Terlevich 1981) diagram and then derived the SFR and SFR/M^* from the spectra taken by the (3 arcsec diameter) SDSS fibre. These SFRs and SFR/M^* were then corrected for aperture biases using galaxy colours measured 'globally', and within the fibre (see B04 for details). Out of the three statistical estimates (mean, median and mode) for the probability distribution of SFR and SFR/M^* derived for each galaxy, we used the median of the probability distribution function (PDF) of the star formation parameters since it is independent of binning.

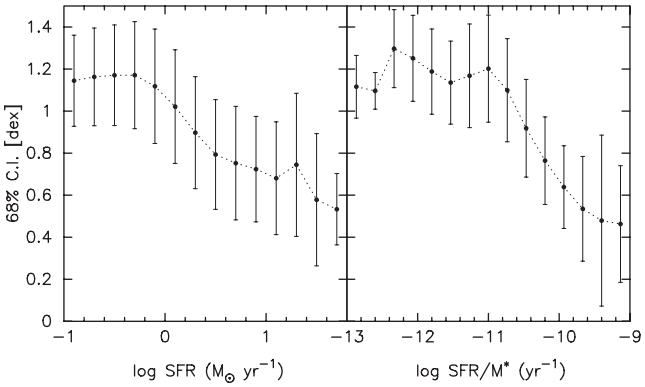

Figure 1. The distribution of the errors on the SFRs of galaxies in our sample. The solid points denote the mean 68 per cent CI of the likelihood distributions for the SFRs in bins of log SFR (left) and log SFR/M^* (right). The error bars show the 2σ scatter in each bin. Galaxies with high SFR have higher S/N in the emission lines, and hence tighter constraints on the estimated SFR and SFR/M^* relative to the galaxies with low or no optical emission. It is also noticeable that the scatter in the CI in all the bins of SFR (and log SFR/M^*) is comparable.

Fig. 1 shows the 68 per cent confidence intervals (CI) for log SFR estimate for each galaxy in our sample and the scatter in CI in bins of log SFR and log SFR/M^*, respectively. The trends are similar to those seen in fig. 14 of B04 (for all galaxies in SDSS DR4). Since the SFR for the star-forming galaxies is measured directly from the high S/N emission lines (>3 in all four lines: Hα, Hβ, [O III] and [N II] required for the BPT diagram), the constraint on the derived value of SFR is tight. However, for the low S/N and non-emission-line galaxies, most of which are passively evolving, SFR is measured indirectly from the 4000 Å break–SFR relation obtained for the high S/N galaxies (see B04 for details), resulting in high uncertainties in the estimated SFR and SFR/M^*. We chose not to select galaxies based on the CI values derived from the probability distribution function of the SFR and SFR/M^* parameters of individual galaxies because excluding galaxies with higher uncertainties in SFR/M^* (or SFR) distribution would exclude a significant number of passive galaxies from the sample. But precautionary measures are taken into account where necessary (Section 2.4), so that our results remain virtually unaffected by the uncertainties in the SFR/M^* (or SFR) estimates for the unclassified galaxies.

2.4 Unclassified galaxies

Any galaxy which cannot be classified using the BPT diagram, because of low S/N or non-detection of the requisite emission lines, is termed 'unclassified' in B04, which makes this class of galaxies rather heterogeneous. The spectra obtained from the 3 arcsec fibre, which encompass ~40–60 per cent of the galaxy's light (at $z \sim 0.1$), may hence only represent the passive core of the galaxy, lacking any emission lines. A careful analysis of the images of these galaxies revealed that these are predominantly bulge-dominated systems, in fact even more concentrated than AGN or composite galaxies

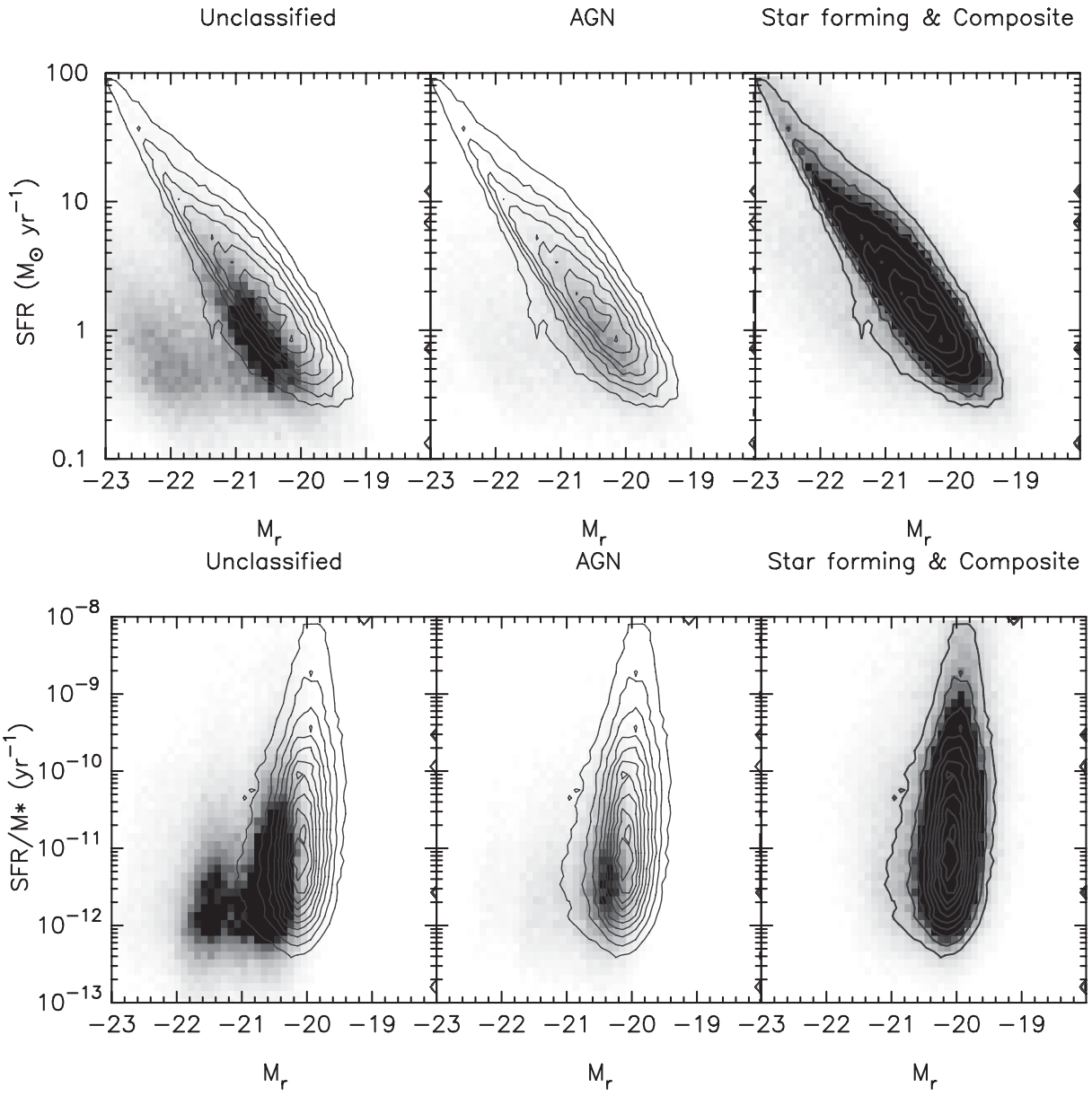

Figure 2. Top: SFR and (bottom) SFR/M^* as a function of r-band magnitude for all the galaxies in SDSS DR4, divided according to their position in the BPT diagram (see Section 2.3). The contours for star-forming+composite class (right-hand panel) are repeated in other panels to compare the relative distributions. The outermost contour in each case represents 100 galaxies per bin, increasing by 100 for every consecutive contour inwards. As expected, the AGN hosts follow the passive galaxy distribution. It is also interesting that the difference between various classes become more distinct for SFR/M^* (bottom panel). These plots show that absolute SFR follows the galaxy luminosity, but the trend reverses when SFR/M^* is considered. Another interesting feature that emerges here is that the observed bimodality in SFR seems to largely consist of the 'non-emission-line' galaxies. This plot gives no indication of enhanced (or suppressed) star formation in AGN hosts, although this might be a result of the obscuration of emission lines by dust around the active nuclei.

(J. Brinchmann, private communication). A detailed investigation of whether all of these galaxies are indeed passively evolving or comprise a sub-population of dust obscured galaxies with an AGN supported star formation in the galactic nucleus is beyond the scope of this work (but see Mahajan & Raychaudhury 2009, where we briefly address related issues).

Fig. 2 shows the distribution of absolute SFR and log SFR/M^* of all galaxies ($-23 \leq M_r \leq -18$) in SDSS DR4 as a function of their luminosity for the three different classes: star forming (and composite), AGN and the unclassified (B04). As previously speculated, the unclassified galaxy class seems to be dominated by passive galaxies. It is also not surprising that the galaxies hosting an AGN, which are known to be bulge-dominated systems, follow the same distribution as that of the unclassified galaxies.

In agreement with previous findings, Fig. 2 shows that most low-luminosity galaxies are efficiently forming stars (Kauffmann et al. 2004; Haines et al. 2006, 2007; Damen et al. 2008; Mahajan et al. 2010). Interestingly, the observed bi-modality in the distribution of SFR is exclusive to the unclassified galaxies. If the SFR of the star-forming galaxies is a function of environment, one should expect the distribution of their SFR to show a bimodal distribution in a data set which samples a wide range of environments, such as that employed here. However, no conclusive remarks can be made on the issue of starburst–AGN connection based on the analysis presented here,

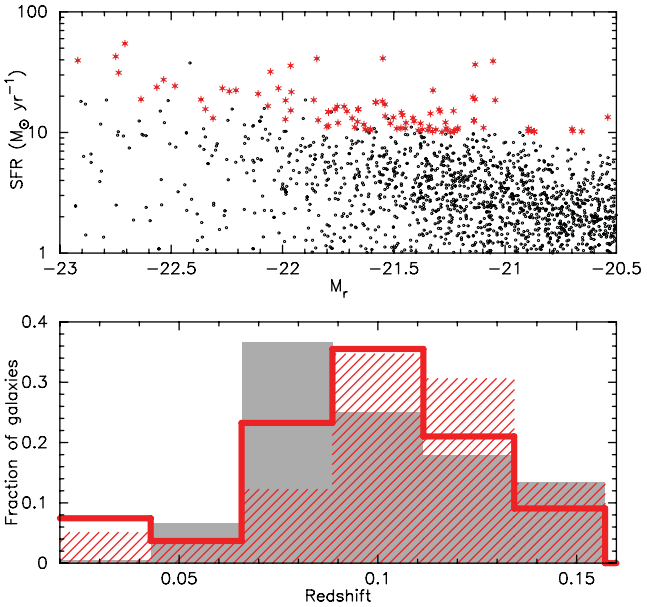

Figure 3. Top: distribution of all (black points) cluster galaxies and starbursts (red stars) within $3r_{200}$ of the cluster centres in the SFR–M_r space shows that the starburst galaxies span the entire magnitude range as spanned by other cluster galaxies. Bottom: the redshift distribution of galaxies in the CN (solid grey) and SB (open red) cluster samples. The KS test does not distinguish between the parent population of these two samples. The red hatched distribution is for the starburst galaxies in the SB sample.

because at visible wavelengths, the circum-nuclear star formation (which largely contributes to the 3 arcsec SDSS fibre spectra) may be entirely obscured by dust enshrouding the active nucleus (e.g. Popescu et al. 2005; Prescott et al. 2007).

2.5 Starburst galaxies

A galaxy having current SFR much higher than that averaged over its past lifetime may be regarded as a starburst. In the context of this paper, dual criteria were adopted to define a starburst galaxy: $\log \mathrm{SFR}/M^* \geq -10\,\mathrm{yr}^{-1}$ *and* $\mathrm{SFR} \geq 10\,\mathrm{M}_\odot\,\mathrm{yr}^{-1}$. These thresholds are purely empirical, driven by the idea of selecting galaxies having current SFR much higher than that averaged over their past star formation history. These limits thus select galaxies contributing to the high end tail of the SFR and SFR/M^* distributions only, as shown in Fig. 3 (top panel).

In particular, they label ∼3 per cent of all and ∼13 per cent of star-forming galaxies in our sample of cluster galaxies as a starburst. In agreement with several other studies (e.g. Feulner et al. 2005; Noeske et al. 2007), we note that by choosing starburst galaxies according to absolute SFR or SFR/M^* alone could bias the selected galaxies to giant or dwarf galaxies, respectively (because dwarf galaxies have higher SFR/M^* than giants but lower absolute SFR; e.g. Damen et al. 2008). These starburst galaxies also cover a wide range in structural properties.

We stress that the above definition of starburst galaxies is used only to sub-classify galaxy clusters in our sample. The results presented in this paper remain unaffected by the specific choice of SFR and SFR/M^* thresholds quantitatively (see Section 3 for a detailed discussion).

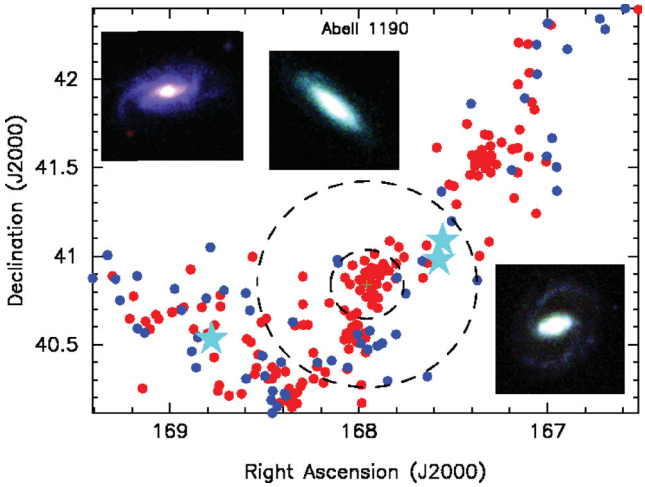

Figure 4. The distribution of red and blue galaxies (colour-selected in the colour–magnitude space; see text) in and around the rich cluster Abell 1190, which is part of our SB sample. The starburst galaxies in its vicinity are shown as cyan *stars* and the corresponding optical images are shown in the inset. The dotted circles represent regions encompassing 1 and 3 Mpc from the centre of the cluster (green cross).

3 STAR FORMATION AND ENVIRONMENT

From a sample of 107 galaxy clusters, those having at least one ($M_r \leq -20.5$) starburst galaxy (as defined in Section 2.5), *anywhere* within 3 Mpc of the cluster centre, were selected, yielding 46 clusters termed as 'SB clusters'. The distance range of 3 Mpc was chosen since, for most of the galaxy clusters in our sample, $r_{200} \sim 1.5$ Mpc. Hence the starburst galaxies chosen to define this sub-class of clusters would either belong to the cluster or to its outskirts. In order to make the selection procedure independent of the uncertainties in the SFR estimate (Section 2.3; Fig. 1), starburst galaxies which are unclassified (Section 2.4) but have estimated $\mathrm{SFR} \geq 10\,\mathrm{M}_\odot\,\mathrm{yr}^{-1}$ in the B04 catalogue were ignored. Redshift distribution of cluster galaxies in the two samples is shown in Fig. 3 (bottom panel). The Kolmogorov–Smirnov (KS) statistic suggests that the two samples are statistically similar. The distribution of redshifts for the starburst galaxies is also statistically similar to that of other cluster galaxies.

A typical SB cluster, Abell 1190, is shown in Fig. 4 as an example. In this figure, galaxies are labelled as red or blue using a colour–magnitude relation fitted to galaxies within 3 Mpc of the cluster centre. Of the rest of the 61 clusters which do not have any starburst galaxy within 3 Mpc of the cluster centre, form the 'comparison' (CN) cluster sample. The fundamental properties of our cluster samples are listed in Tables 1 and 2, respectively. In total 3966 galaxies are found within $3r_{200}$ of the cluster centres, of which 3903 are non-AGN and were used for all further analysis, unless stated otherwise. If the occurrence of starburst galaxies in some clusters is purely coincidental, or the result of line-of-sight (LOS) superposition, then CN and SB cluster samples should display similar properties. As shown below, this hypothesis fails to hold.

3.1 The last 'bursts' of star formation

The 4000 Å break (D_n4000) is a prominent discontinuity occurring in the continuum of the visible spectrum of a galaxy. It arises because a large number of absorption lines, mainly from ionized metals, accumulate in a small wavelength range. In hot young stars, the

Table 1. Abell clusters with starburst galaxies on outskirts (SB).

Abell	RA (J2000)	Dec. (J2000)	Richness	z	Velocity dispersion (σ_v; km s^{-1})
152	1 9 50.0	+13 58 45	0	0.0581	756
175	1 19 33.0	+14 52 29	2	0.1288	705
628	8 10 9.5	+35 12 28	0	0.0838	741
646	8 22 12.0	+47 5 44	0	0.1303	849
655	8 25 23.1	+47 6 32	3	0.1267	858
714	8 54 50.2	+41 54 0	1	0.1397	609
724	8 58 20.4	+38 33 48	1	0.0934	492
856	9 45 30.1	+56 32 43	0	0.1393	450[a]
874	9 50 43.8	+58 1 29	1	0.1480	1551
941	10 9 42.7	+3 40 56	1	0.1049	195
971	10 19 49.6	+40 57 34	1	0.0929	873
975	10 22 47.3	+64 37 29	2	0.1182	273
1004	10 25 36.5	+51 3 23	1	0.1414	963
1021	10 28 45.2	+37 39 21	1	0.1114	828
1076	10 45 9.5	+58 9 55	1	0.1164	507
1132	10 58 25.5	+56 47 41	1	0.1363	792
1190	11 11 49.2	+40 50 30	2	0.0752	693
1227	11 21 38.4	+48 2 22	2	0.1120	813
1238	11 22 58.6	+ 1 6 21	1	0.0733	552
1341	11 40 35.8	+10 23 18	1	0.1050	834
1342	11 40 41.8	+10 4 18	1	0.1061	390
1346	11 41 10.9	+ 5 41 18	1	0.0976	711
1354	11 42 11.7	+10 9 14	1	0.1178	456
1373	11 45 27.8	− 2 24 40	2	0.1314	627
1377	11 47 2.4	+55 44 16	1	0.0511	684
1424	11 57 34.1	+ 5 2 14	1	0.0774	699
1446	12 1 55.9	+58 1 14	2	0.1031	747
1496	12 13 26.2	+59 16 19	1	0.0937	396
1518	12 19 3.9	+63 30 24	0	0.1080	783
1534	12 24 7.5	+61 30 26	0	0.0698	321
1544	12 27 46.3	+63 25 25	1	0.1454	597
1713	13 19 11.8	+58 5 22	1	0.1406	1095
1738	13 25 9.7	+57 36 35	2	0.1155	597
1750	13 30 52.4	− 1 51 6	0	0.0855	795
1896	14 18 40.9	+37 48 27	0	0.1329	534
1999	14 54 5.6	+54 20 5	1	0.0994	333
2026	15 8 33.8	− 0 15 51	1	0.0875	753[b]
2051	15 16 46.4	− 0 56 28	2	0.1155	600
2053	15 17 15.8	− 0 40 23	1	0.1127	831
2142	15 58 16.3	+27 13 53	2	0.0894	942
2149	16 1 37.9	+53 52 57	0	0.1068	723
2183	16 21 31.6	+42 43 20	1	0.1366	495
2197	16 28 10.3	+40 54 47	1	0.0301	564
2199	16 28 36.8	+39 31 48	2	0.0299	759
2244	17 2 44.2	+34 4 13	2	0.0970	1164
2255	17 12 30.5	+64 5 33	2	0.0809	1116

[a] Popesso et al. (2007).
[b] Popesso et al. (2007).

Table 2. Comparison (CN) clusters.

Abell	RA (J2000)	Dec. (J2000)	Richness	z	Velocity dispersion (σ_v; km s^{-1})
190	1 23 41.9	− 9 51 30	0	0.1015	354
612	8 1 4.0	+34 48 2	1	0.0774	186
667	8 28 6.0	+44 42 23	0	0.1450	792
671	8 28 31.0	+30 24 26	0	0.0503	801
690	8 39 16.0	+28 49 50	1	0.0788	516
695	8 41 26.1	+32 16 40	1	0.0687	375
775	9 16 21.2	+ 5 52 2	1	0.1340	975
819	9 32 17.9	+ 9 39 18	0	0.0764	561
858	9 43 26.6	+ 5 52 52	0	0.0881	918
990	10 23 33.8	+49 9 30	1	0.1440	1041
1024	10 28 18.5	+ 3 45 21	1	0.0743	690
1038	10 32 59.4	+ 2 15 17	1	0.1246	297
1064	10 38 46.9	+ 1 16 4	1	0.1320	594
1068	10 40 50.2	+39 57 1	1	0.1386	1317
1080	10 43 58.8	+ 1 5 0	0	0.1205	432
1139	10 58 4.9	+ 1 30 45	0	0.0395	249
1169	11 8 10.0	+43 56 34	1	0.0587	591
1171	11 7 29.2	+ 2 56 31	0	0.0757	159[a]
1173	11 9 14.4	+41 34 33	1	0.0759	570
1205	11 13 23.0	+ 2 30 29	1	0.0759	810
1225	11 21 24.5	+53 46 22	0	0.1040	732
1270	11 29 33.3	+54 4 20	0	0.0686	600
1302	11 33 30.4	+66 25 18	2	0.1160	834
1318	11 36 30.6	+54 58 16	1	0.0564	366
1361	11 43 48.3	+46 21 17	1	0.1167	453
1364	11 43 39.8	− 1 46 36	1	0.1063	558
1368	11 45 1.7	+51 15 13	1	0.1291	762
1372	11 45 29.3	+11 31 13	1	0.1126	435
1383	11 48 13.5	+54 37 12	1	0.0600	426
1385	11 48 5.5	+11 33 16	1	0.0831	531
1387	11 48 54.1	+51 37 12	1	0.1320	753
1390	11 49 35.1	+12 15 15	0	0.0829	342
1402	11 52 37.4	+60 25 15	0	0.1058	219
1452	12 3 42.6	+51 44 14	0	0.0628	513[b]
1552	12 29 50.6	+11 44 29	1	0.0859	711
1559	12 33 10.0	+67 7 31	1	0.1066	693
1564	12 34 57.3	+ 1 51 32	0	0.0792	687
1566	12 35 5.1	+64 23 32	2	0.1000	561
1577	12 37 52.0	− 0 16 22	1	0.1405	366
1621	12 48 45.9	+62 41 46	1	0.1029	534
1630	12 51 44.8	+ 4 34 49	1	0.0648	426
1637	12 53 59.3	+50 49 51	1	0.1270	564
1646	12 55 48.6	+62 9 53	0	0.1063	468
1650	12 58 46.1	− 1 45 57	2	0.0845	513
1663	13 2 46.4	− 2 31 49	1	0.0847	891
1764	13 34 43.2	+59 55 51	0	0.1167	585
1773	13 42 8.5	+ 2 15 7	1	0.0766	1098
1780	13 44 38.1	+ 2 53 12	1	0.0786	426
1882	14 14 39.8	− 0 20 33	3	0.1367	612
1885	14 13 47.6	+43 40 15	1	0.0890	1038
1918	14 25 9.2	+63 9 41	3	0.1394	1008
1920	14 27 17.5	+55 46 46	2	0.1310	570
1936	14 34 28.8	+54 50 5	1	0.1386	498
2018	15 1 12.8	+47 16 26	1	0.0872	1029
2046	15 12 41.4	+34 51 9	1	0.1489	948
2062	15 21 19.8	+32 5 38	1	0.1155	537
2110	15 39 43.5	+30 42 45	1	0.0980	654
2175	16 20 23.1	+29 55 18	1	0.0972	876
2196	16 27 21.6	+41 29 43	0	0.1332	687
2211	16 34 4.0	+40 57 9	1	0.1355	537
2245	17 2 45.0	+33 33 13	1	0.0852	984

[a] Popesso et al. (2007).
[b] Struble & Rood (1999).

metals are multiply ionized and hence the opacity is low, resulting in a smaller D_n4000 relative to old, metal-rich stars. We used the same definition of D_n4000 as adopted by B04, which is the ratio of average flux density in the narrow continuum bands (3850–3950 and 4000–4100 Å). This definition was initially introduced by Balogh et al. (1999) and is an improvement over the original definition of Bruzual (1983) in the sense that the narrow continuum bands make the index considerably less sensitive to reddening effects.

The Hδ absorption line occurs when the visible light of a galaxy mainly comes from late-B and early-F stars. A large absorption in Hδ implies that a galaxy experienced a major burst of star

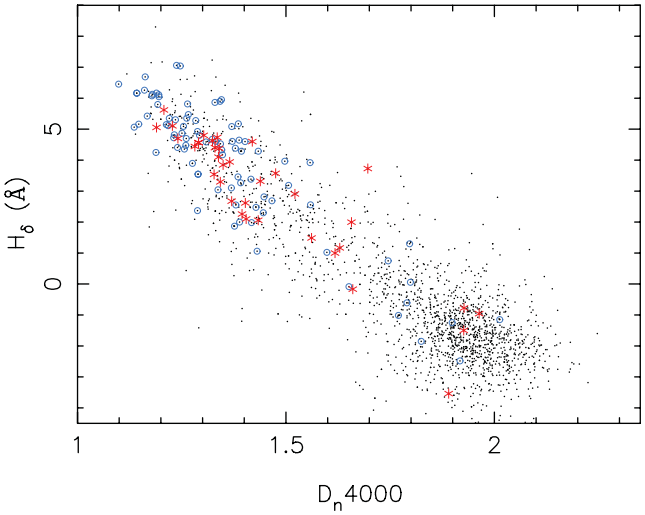

Figure 5. All galaxies in the SB clusters are plotted as black dots in the D_n4000–Hδ space. Overplotted as red stars are starburst galaxies found at $1 \leq r/r_{200} \leq 2$. The blue circles are galaxies at the same distance from the cluster, but having $1 \leq \mathrm{SFR} < 10\,\mathrm{M}_\odot\,\mathrm{yr}^{-1}$. Most of these infalling galaxies with high SFR (and SFR/M^*) occupy the area in the D_n4000–Hδ space where galaxies with currently ongoing or recent starbursts are expected to lie (Kauffmann et al. 2004).

formation ∼0.1–1 Gyr ago, while a stronger D_n4000 is an indicator of metal-rich ISM. Hence together EW(Hδ) and D_n4000 indicate whether a galaxy has been forming stars continuously [intermediate/high D_n4000 and low EW(Hδ)] or in bursts [low D_n4000 and high EW(Hδ)] over the past Gyr (Kauffmann et al. 2003). Fig. 5 shows the distribution of spectacular starburst galaxies (SFR $\geq 10\,\mathrm{M}_\odot\,\mathrm{yr}^{-1}$ & $\log \mathrm{SFR}/M^* \geq -10\,\mathrm{yr}^{-1}$) relative to all other galaxies in the SB cluster sample, in the D_n4000-Hδ plane. It is clear that our adopted criteria for defining starburst galaxies on the basis of integrated SFR and SFR/M^* segregate these galaxies well in the space defined by spectral indices sensitive to recent star formation. For a comparison, we also show galaxies which have the same SFR/M^* but absolute SFR which is up to 10 times lower than that of 'starburst' galaxies. For the latter, the distribution shows a larger scatter.

3.2 Starburst galaxies on the outskirts of clusters

We began this section by sub-classifying clusters on the basis of the presence of starburst galaxies in them. In order to test the hypothesis that these starburst galaxies might occur randomly within a cluster, we plot the first, square root of the second and the third moment (mean, standard deviation and skewness) of SFR, respectively, as a function of (scaled) cluster-centric radius, in Fig. 6. We extend our analysis up to 3 r_{200} because it encompasses the core of the galaxy cluster and its outskirts (Diaferio & Geller 1997; Lewis et al. 2002; Gómez et al. 2003), providing a range of galactic environments to explore.

The SFR profiles of the two samples in Fig. 6 are strikingly different, with SB clusters showing a higher mean SFR relative to CN clusters at almost all radius. The striking feature of this stacked SFR profile is the sudden increase in the standard deviation in SFR, which, accompanied by positive skewness, indicates an enhancement in the mean star formation of galaxies in the SB clusters. This

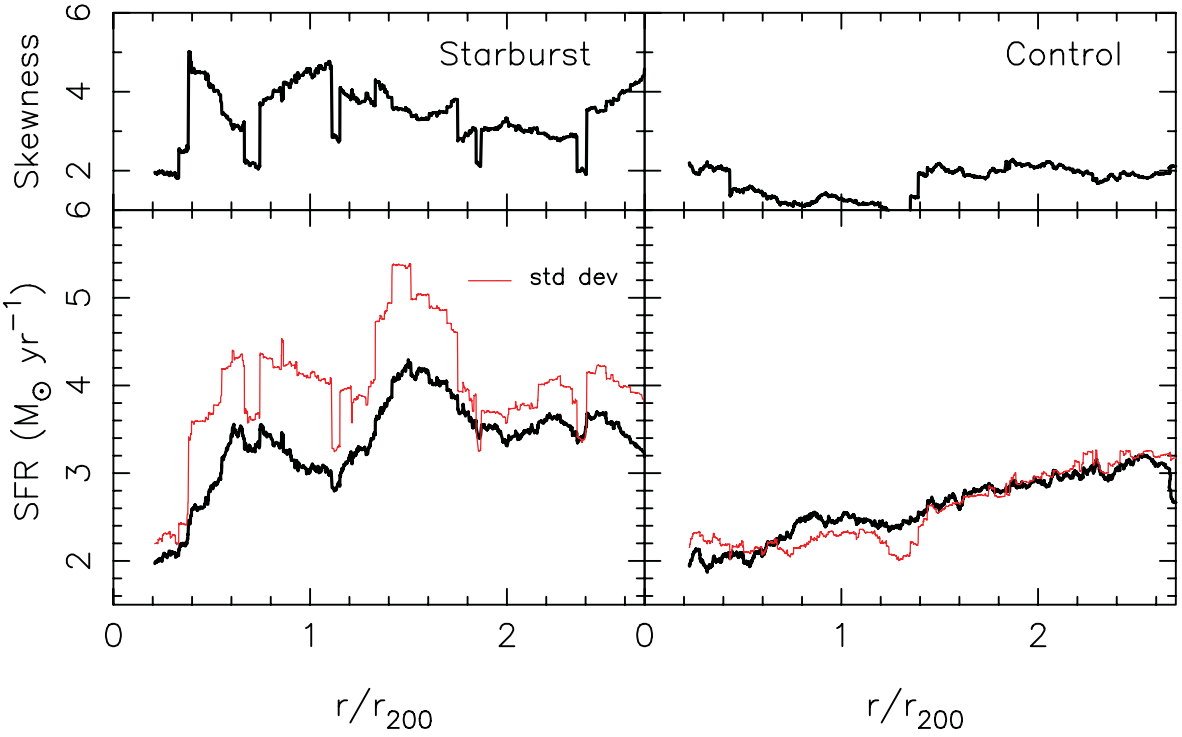

Figure 6. The mean (thick line, bottom panel), skewness (upper panel) and standard deviation (thin red, bottom panel) in SFR of galaxies in SB (left) and CN (right) clusters in running bins (250 galaxies per bin) of (scaled) cluster-centric radius. Unclassified galaxies with $\mathrm{SFR} > 10\,\mathrm{M}_\odot\,\mathrm{yr}^{-1}$ and AGN were excluded. As expected, the SFR falls towards the cluster centre. But the difference in the SFR profiles of the two samples is striking. The high standard deviation at the cluster boundary ($r \sim r_{200}$) indicates the presence of galaxies with extreme SFRs. It is also noticeable that the mean SFR of CN clusters is lower than that of SB clusters in general.

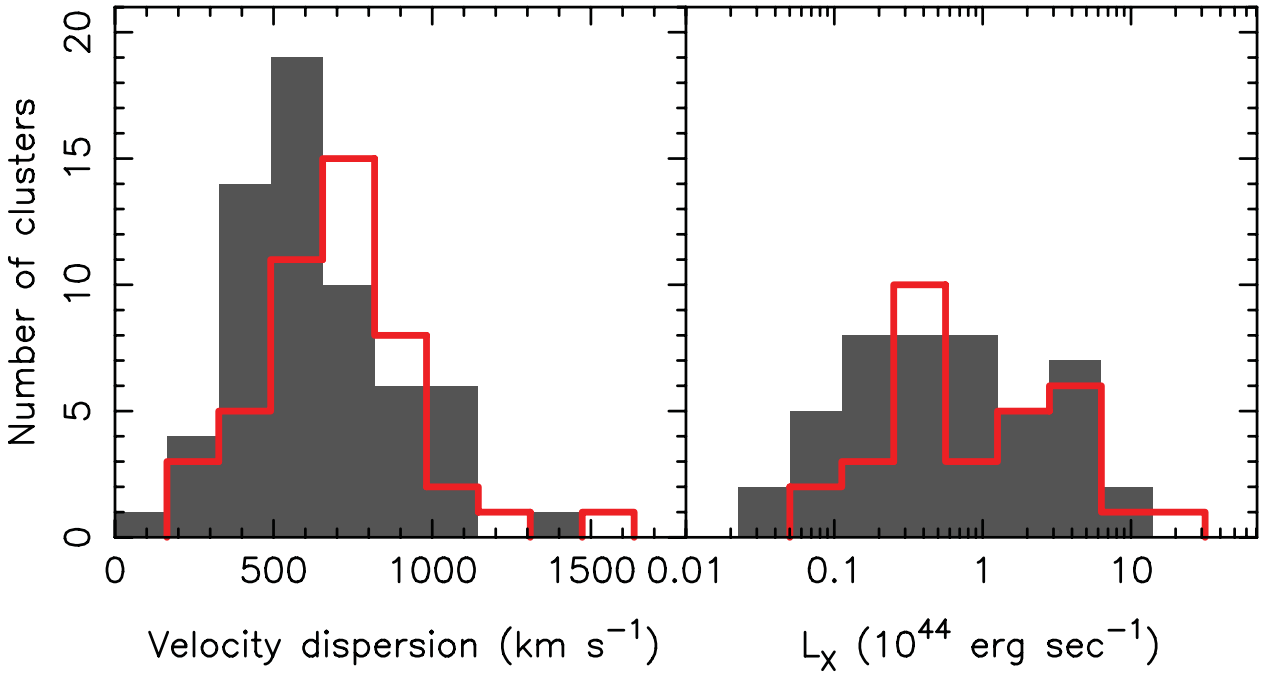

Figure 7. The velocity dispersion (left) and X-ray luminosity (L_X) (right) distribution of SB (red open) and CN (grey solid) cluster samples, respectively. The L_X are available for almost 70 per cent of both samples. While the SB clusters are found to have systematically higher velocity dispersions than the CN clusters, the distribution of L_X shows no significant statistical differences, suggesting that the SB clusters although not more massive than their CN counterparts are dynamically more unrelaxed.

shows that several highly star-forming galaxies are present just outside the boundary ($\sim 1.5 r_{200}$) of SB clusters. Given that the selection criteria demanded that starburst galaxies could occur in these clusters anywhere within the given threshold (3 Mpc), it seems highly unlikely that occurrence of such a 'blip' is a random chance. There seems to be another region of increase in the mean SFR of galaxies in the SB clusters at $\sim 0.5\, r_{200}$. We note that the latter feature, closer to the cluster core, is neither due to the presence of group-like structures ($\sigma_v \leq 300\,\mathrm{km\,s^{-1}}$; Table 1) nor due to the nearby interacting cluster pair Abell 2197 and 2199 present in our sample. Both these features in the SFR profile of SB clusters are thus considered real. We discuss them in detail in the following sections.

3.3 Clusters and filaments

In order to explore whether the enhancement in SFR of galaxies found on cluster outskirts (Section 3.2) is related to the properties of the clusters themselves, the distribution of velocity dispersion (σ_v) and X-ray luminosities (L_X), where available, for the two cluster samples are plotted in Fig. 7. Since σ_v are derived from spectroscopic redshifts using an iterative procedure (ROSTAT; Beers et al. 1990), the error in individual σ_v values is very small. L_X are obtained for 31/46 SB and 45/61 CN clusters, respectively, from Base de Données Amas de Galaxies X (BAX; http://bax.ast.obs-mip.fr/), which is an online data base providing observational X-ray measurements for clusters of galaxies observed by various space- and ground-based X-ray missions. In the following we use L_X measured in the 1.5–2.4 keV energy band as a proxy for cluster mass, and σ_v as a proxy for the dynamical state of the cluster.

Fig. 7 shows that despite the fact that cluster samples consist of a wide range of objects (group-like structures to massive clusters), their σ_v distributions are significantly different. As suggested by the KS statistic, SB clusters have higher σ_v than CN clusters, but there are no statistical differences in the distributions of the L_X for the two samples. To confirm that we are not selecting only the X-ray bright clusters in either of the samples, we further checked that the σ_v distributions of clusters from the two samples, for which L_X are not available, are not statistically different, as confirmed by the KS test. This implies that there is no difference in the mass distribution of the two samples. However, similar L_X but higher σ_v suggest that the SB clusters are likely to be dynamically unrelaxed relative to the CN sample. The observed difference in the σ_v distribution is not due to the two sample of clusters being sampled from different ranges of redshift since both the cluster samples cover a redshift range (0.02–0.15) spanning only $\sim$1.5 Gyr in lookback time.

If a cluster is being assembled via galaxies falling in through large-scale filaments, the unrelaxed dynamical state of the cluster will be observable as high σ_v, especially if one or more such filaments align along the LOS. Hence the above observations could be interpreted as the manifestation of systematic differences in the dynamical state of the two cluster samples with similar mass distributions. Such an impact of the global environment, in which a galaxy is embedded, on its star formation properties, is inevitable (e.g. Porter & Raychaudhury 2007; Fadda et al. 2008; Porter et al. 2008; Edwards et al. 2010a; Haines et al. 2011). However, an interesting question is whether the large-scale structure directly influences the evolution of galaxies therein, or has an indirect effect. Here, we use the position of galaxies along the cosmic web to explore this further. The catalogue of galaxy filaments used in this paper is sourced from SDSS DR4 by using the algorithm described by Pimbblet, Drinkwater & Hawkrigg (2004, hereafter PDH04).

Just as in PDH04, all filaments are classified into morphological classes from types I to V, i.e. straight, warped, sheet-like, uniform and irregular distribution of galaxies, respectively, with respect to an inter-cluster axis. The algorithm is well described in PDH04, but for the benefit of the readers we briefly describe it here: to identify

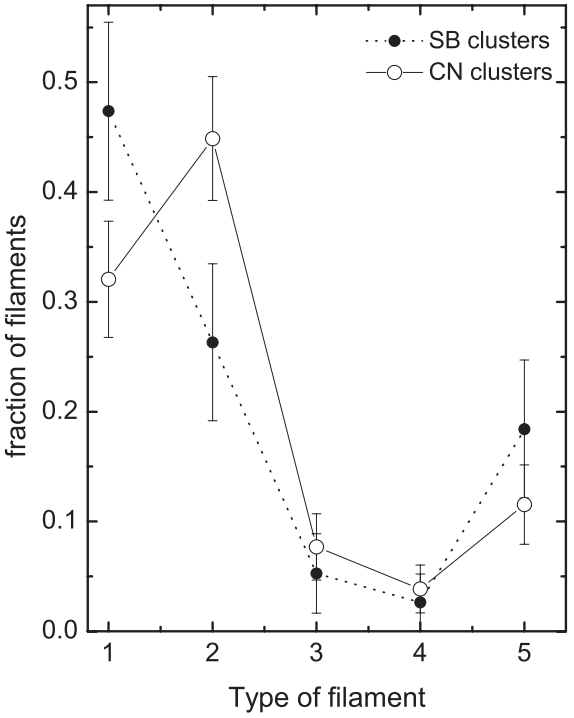

Figure 8. The distribution of the morphological type of filament (according to the PDH04 classification) for the 'clean' filaments in the SB (dotted) and CN (solid) cluster samples, respectively. The errors are calculated using equation (3). The SB and CN clusters show significantly different preferences for type I and type II filaments, respectively.

galaxy filaments in a large-scale survey such as the SDSS involved setting up orthogonal planar pair projections of the filaments viewed along the inter-cluster axis. The planes corresponded to ± 20 Mpc from the inter-cluster axis and had a depth of ± 5 Mpc around it. This choice of depth and width ensures that the ability to visualize highly curved and complex filaments is retained (fig. 1 of PDH04 illustrated this process in more detail). Finally, those filaments for which both Mahajan and Pimbblet agreed on the same morphological class were included in the 'clean' sample, and were used in all further analysis.

Simulations have shown that properties, such as matter density of filaments, are closely related to their morphology (Colberg, Krughoff & Connolly 2005; Dolag et al. 2006). Therefore, by studying the morphology of filaments through which a galaxy approaches the cluster, we intend to explore how, if at all, is the LSS modulating galaxy evolution. Fig. 8 shows the distribution of morphological type of filaments belonging to both the cluster samples. The errors were calculated using binomial statistics, where, if within a fixed radial range, n out of N clusters in a given sample had a particular type of filament feeding them, then the likelihood of a cluster to have that class of filament is given by $L \propto f^n(1-f^n)^{N-n}$ (De Propris et al. 2004). The error on the fraction of clusters is given by the standard deviation

$$\Delta f_x = \sqrt{\frac{n(N-n)}{N^3}}. \quad (3)$$

Each distribution was normalized to unity. The number of filaments classified for each cluster sample is listed in Table 3. The choice of the magnitude cut of $M_r \leq -20.5$ excludes all low-luminosity galaxies from the analysis, thus significantly underestimating the density of some of the galaxy filaments. Hence the morphological class for a large fraction of the galaxy filaments could not be determined by the visual inspection of density contours on the projected planes. On the other hand, this also implies that the uncertainty in determining the morphological class of the 'clean' filament sample is very small.

Table 3. Type of filaments.

Sample	I	II	III	IV	V	Undetermined
SB	18	10	2	1	7	47
CN	25	35	6	3	9	68

Fig. 8 suggests that the CN clusters are more likely to be fed by type II (warped) filaments. The number of filaments associated with individual clusters does not show any particular trend.

4 DISCUSSION

Superclusters are the most massive and youngest structures in the Universe within which groups and clusters of galaxies evolve through interactions and mergers. In this hierarchical model, clusters are assembled by accreting surrounding matter in the form of galaxies and galaxy groups (e.g. Bekki 1999; Struck 2006; Oemler et al. 2009) through large-scale filaments (Zeldovich, Einasto & Shandarin 1982; Colberg et al. 2000; Porter & Raychaudhury 2007; Fadda et al. 2008; Porter et al. 2008; Edwards et al. 2010a). On the course of their journey from the sparsely populated field to the dense cores of clusters, galaxies encounter a range of different environments, under the influence of which they evolve, not only by exhausting their gas content in forming stars, but also by losing the gas to their surroundings. Thus, one of the most crucial links required to fully understand galaxy evolution is to find how do the galaxies in cluster cores become passive while those in the field remain star forming.

4.1 Excessive star formation on the outskirts of clusters

Studies to understand the evolution of galaxies in various environments generally involve large-angle sky surveys (e.g. Kauffmann et al. 2004), or target particular environments (Gavazzi et al. 2003; Balogh et al. 2004; Mercurio et al. 2004; Rines et al. 2005; Verdugo, Ziegler & Gerken 2008). Despite the well-known dominance of passively evolving galaxies in clusters, several starburst galaxies have been serendipitously discovered near the boundaries of intermediate-redshift clusters ($z \geq 0.2$; Keel 2005; Moran et al. 2005; Sato & Martin 2006; Marcillac et al. 2007; Fadda et al. 2008; Oemler et al. 2009), as well as in the local Universe (Sun & Murray 2002; Gavazzi et al. 2003; Cortese et al. 2007; Reverte et al. 2007). An interesting question then is whether the occurrence of such starburst galaxies in some clusters is by chance, or do they constitute a missing link in understanding galaxy evolution and the assembly of the cosmic web.

In a study of inter-cluster filaments derived from the 2dFGRS, Porter & Raychaudhury (2007) and Porter et al. (2008) found that the mean SFR of galaxies ($z < 0.1$) in inter-cluster filaments increases at $\sim$3 Mpc from the cluster centre. However, due to the unavailability of requisite data for separating AGN from star-forming galaxies, and of SFRs derived using sophisticated algorithms,[1] their

[1] Porter & Raychaudhury (2007) and Porter et al. (2008) used a statistical quantity, the η-parameter from the 2dFGRS data base, which is derived from the principal component analysis of the spectra as a proxy (Madgwick et al. 2002).

results had some inherent uncertainties. Their results found support in observations of extended fields around lensing clusters, where Moran et al. (2005), for example, had found that all of their [O II] emitting galaxies in CL0024 ($z = 0.4$) lie around the virial radius of the cluster. Considering a simple infall model, Moran et al. (2005) deduced that the observed excess in the [O II] emitters at the cluster's periphery can be explained in a scenario whereby an early-type galaxy on its infall experiences a burst of star formation at the virial radius lasting 200 Myr and contributing 1 per cent of the total galaxy mass. They attributed the burst of star formation to interaction of galaxies with shocks in the ICM or the onset of galaxy–galaxy harassment.

Using the SDSS and 2dFGRS spectroscopic data for galaxies, Balogh et al. (2004) found a critical local projected density of $\Sigma_5 \sim 2\,\mathrm{Mpc}^{-2}$ in the SFR–density relation characterized by the near complete absence of galaxies with large EW(Hα) at densities greater than that (see their fig. 3). This critical density is similar to that found near the cluster boundary ($\sim$2–3$h^2\,\mathrm{Mpc}^{-2}$; Rines et al. 2005).

By analysing a sample of close galaxy pairs in the SDSS, Sol Alonso et al. (2006) have suggested that galaxy–galaxy interactions are most efficient in inducing a burst of star formation when the projected distance between galaxies is $\sim$100 kpc and their relative velocity is $\sim$350 km s^{-1}. Furthermore, they found that these conditions are most effective in low-/intermediate-density environments. The conditions just outside the cluster boundary are thus well suited for galaxies to tidally influence each other. However, given the complicated kinematics involved, galaxies do not have enough time to merge together, as they progressively drift towards the cluster core with an additional effective infall velocity of $\sim$220–900 km s^{-1}. For instance, even for a broad range of cluster masses $10^{12} \leq M_{\mathrm{clus}} \leq 10^{15}\,\mathrm{M}_{\odot}$, Pivato, Padilla & Lambas (2006) find that the maximum infall velocity occurs in a narrow cluster-centric radial range of $2 < r_{\mathrm{max}} < 6$ Mpc.

If the dominant process is galaxy–galaxy harassment in the infall regions of clusters, successive high speed encounters between galaxies will lead to the inflow of gas towards the central regions of the harassed (mostly low-mass) galaxies (e.g. Fujita 1998). Lake, Katz & Moore (1998), for instance, showed that most of the fuel for star formation in a harassed galaxy may be driven to the central kpc of a galaxy within 1–2 Gyr in such interactions, and in many cases in their simulations, half of the gas mass was transferred to the core of such a galaxy in <200 Myr. This will cause rapid star formation in the core, and of course, if the galaxy is massive enough to have an AGN, it might be fuelled as well. In Fig. 9, we present a montage of some of the 'starburst' galaxies within a radial distance of 1–2 r_{200} of the centres of our SB clusters, where we have used $g'r'i'$ images from the SDSS archive and produced 'true colour' images. We can see that these galaxies represent a wide variety of morphologies, though they seem to be predominantly disc galaxies, and many have close neighbours. What is striking from these images is that most have concentrated nuclear star formation, which is indicative of such processes in action. One caveat is that our galaxies were chosen on the basis of spectra obtained with fibres, so, barring the farthest galaxies in the sample, many spectra have preferentially sampled the central regions of these galaxies.

The density of the ICM at the periphery of clusters is small. Hence, any cluster related environmental process that could directly influence the infalling galaxies can be ruled out as a cause of enhancement in the SFR of galaxies (but see Kapferer et al. 2009, whose simulations suggest that under some particular conditions the ICM density on cluster outskirts is enough for ram-pressure stripping of infalling galaxies). The local conditions on the outskirts of clusters, i.e. small relative velocities between pairs of galaxies, and higher galaxy density with respect to the field, seem to favour interactions among galaxies, and may lead to the observed enhancement in the SFR of galaxies in these regions. Several other observational studies (Lewis et al. 2002; Balogh et al. 2004; Moran et al. 2005; Sol Alonso et al. 2006; Porter & Raychaudhury 2007; Porter et al. 2008) and simulations (Fujita 1998; Gnedin 2003) have also concluded that galaxy–galaxy interactions are the most suitable explanation for the observed differences between galaxies in and around clusters, and those in the field.

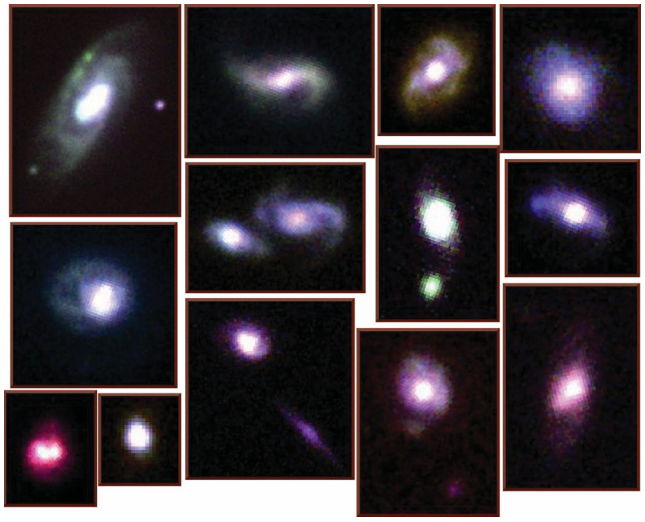

Figure 9. True colour SDSS images of some of the typical starburst galaxies found on the outskirts (1–2r_{200}) of SB clusters in g', r' and i' filters (represented by red, green and blue colours, respectively). These galaxies cover a wide range in morphologies, and some show structural deformities and the presence of close neighbours. The star-forming regions are predominantly nuclear, but this might not be surprising since the star formation rate is based on fibre spectra.

The 'blip' near r_{200} in the mean SFR profile of SB clusters (Fig. 6) could be a result of these short-time interactions. As a galaxy approaches the core of the cluster into which it is falling, it begins to experience the dynamical and tidal influence of the residual substructure in the cluster (Gnedin 2003). We would like to stress that the reason such a trend has not been widely noticed is that it is very difficult to detect and quantify the enhancement in the star formation activity, occurring on such small time-scales and confined to such narrow regions on sky (Pivato et al. 2006; Porter et al. 2008). Thus, it is not surprising that despite stacking a fairly significant sample of clusters, only a subdued signal was detected here.

Fig. 10 provides some more insight into the difference in the SFR profile of the SB and CN clusters. A comparison of the fraction of star-forming galaxies as a function of the cluster-centric radius for the two samples shows that the fraction of starburst galaxies is higher in the SB clusters at almost all radius, irrespective of how the star-forming galaxies are selected. This evidently shows that the CN clusters are likely to be dynamically relaxed, virialized systems, where the total rate of star formation is lower than the SB clusters.

The other peak in the mean SFR profile (Fig. 6), observed nearer the cluster centre, could be a consequence of the onset of the cluster-related processes such as ram-pressure stripping, or it could be the result of an alignment of several cluster-feeding filaments along the LOS. While the confirmation of latter requires data at other

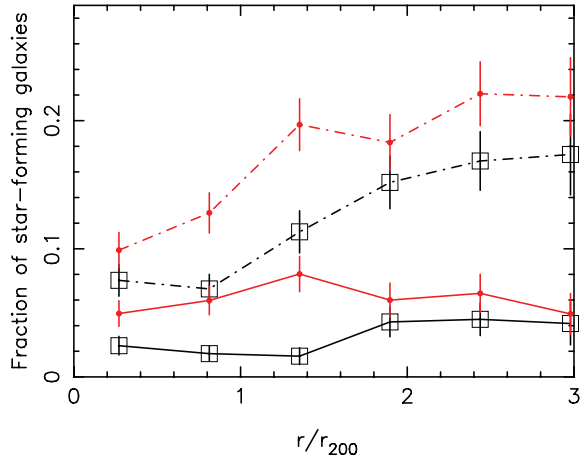

Figure 10. Fraction of star-forming galaxies in the SB (red circles) and CN (black squares) cluster samples, respectively, as a function of scaled cluster-centric distance. The distributions shown by solid lines correspond to the selection of star-forming galaxies as log SFR/M^* $\geq -10.5\,\mathrm{yr}^{-1}$ and SFR $\geq 10\,\mathrm{M}_{\odot}\mathrm{yr}^{-1}$, while for the dot–dashed lines the criteria are log SFR/M^* $\geq -10\,\mathrm{yr}^{-1}$ and SFR $\geq 1\,\mathrm{M}_{\odot}\mathrm{yr}^{-1}$, respectively. The fraction of star-forming galaxies in the CN clusters is almost always lower than the SB clusters, irrespective of how star-forming galaxies are selected.

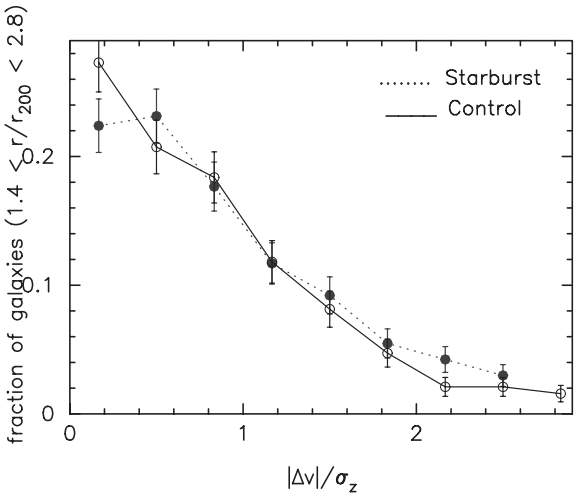

Figure 11. Fraction of galaxies ($1.4 \leq r/r_{200} \leq 2.8$) in the SB (dotted) and CN (solid) cluster samples as a function of scaled relative velocity. No significant peak at 0 or above implies that these galaxies are a mix of infalling and backsplash galaxies (Gill, Knebe & Gibson 2005).

wavelengths and sophisticated modelling, the former can only be tested in simulations. We leave this issue for later consideration.

Kauffmann et al. (2004, their fig. 12) showed that the D_n4000 feature in star-forming galaxies is well correlated with the internal extinction (measured in the SDSS z band). For $D_n4000 \sim 1$ (most of our galaxies have $D_n4000 \gtrsim 1$; see Fig. 5), the internal extinction can be as high as 1.5 mag (in the z band). Hence, it is very likely that the number of starburst galaxies observed at visible wavelengths may be severely underestimated, making observations of this phenomenon even more difficult with data in one wavelength regime alone (also see Gavazzi et al. 2003; Mahajan & Raychaudhury 2009; Wolf et al. 2009; Mahajan et al. 2010).

A cluster with a deep potential well attracts relatively more galaxies compared to one with a shallower potential, which implies that the increased galaxy density on the outskirts of a cluster implies higher probability for galaxy–galaxy interactions in more massive clusters. In the literature, however, there seems to be ambiguity in the observational results. In a study of 25 clusters ($0 < z \leq 0.8$), Poggianti et al. (2006) found that although the fraction of emission-line galaxies is anti-correlated with the cluster's σ_v at high redshift, the intermediate mass ($\sigma_v \sim 500$–$600\,\mathrm{km\,s}^{-1}$) $z \sim 0$ clusters do not show any systematic trend. Biviano et al. (1997) showed that at $z \leq 0.1$ the fraction of emission-line galaxies is higher by ∼33 per cent in clusters with $\sigma_v < 600\,\mathrm{km\,s}^{-1}$ as compared to those with $\sigma_v > 900\,\mathrm{km\,s}^{-1}$. On the other hand, in a study of 17 clusters from the 2dFGRS, Lewis et al. (2002) found no difference between the mean luminosity normalized SFR (proxy for specific star formation rate) profile of their clusters separated around $\sigma_v = 800\,\mathrm{km\,s}^{-1}$. In this paper, using L_X as a proxy for the mass for almost 70 per cent of our clusters, we do not find any difference in the mass distribution of the two samples, but we find the distributions of the σ_v to be significantly different. We believe this is because σ_v represents the dynamical state of a cluster, i.e. the degree of relaxation, rather than the mass of the cluster, as is often used in the literature.

It might be argued that the observed enhancement in the SFR of galaxies, on the periphery of clusters, is due to the mixing of 'backsplash' galaxies (e.g. Gill et al. 2005; Mahajan, Mamon & Raychaudhury 2011b, and references therein) with those falling into the cluster for the first time. This 'backsplash' population comprises galaxies which have crossed the cluster core at least once and are observed on the other side of its periphery (Balogh, Navarro & Morris 2000; Mamon et al. 2004; Gill et al. 2005; Rines et al. 2005). In their simulation, Gill et al. (2005) showed that backsplash galaxies can be detected by their distinct centrally peaked velocity dispersion distribution in the radial interval 1.4–$2.8r_{200}$, while a non-zero velocity distribution peak shows that the galaxies are falling into the cluster for the first time.

This hypothesis was tested by plotting the distribution of the relative LOS velocities of galaxies in the interval 1.4–$2.8r_{200}$. The distribution for SB (and CN) cluster samples, as shown in Fig. 11, showed no prominent peak at $|\Delta v|/\sigma_z = 0$. This implies that the galaxies in the infall regions of the cluster samples studied here are a mix of infall and backsplash populations. This is in agreement with earlier studies (Rines et al. 2005; Pimbblet et al. 2006) confirming that some emission-line galaxies in and around clusters are a result of backsplash, but a pure backsplash model does not explain all their properties. Using simple models on similar data, Mahajan et al. (2011b) have shown that even a single passage through the cluster core is enough to completely quench the star formation in a galaxy.

Earlier studies showed that SB galaxies in distant ($z \sim 0.5$) clusters are likely to be low-luminosity dwarfs (Poggianti et al. 1999). As mentioned before, in the observation of enhanced [O II] emission at 1.8 Mpc from the centre of CL0024 ($z = 0.4$; Moran et al. 2005), all of the emission-line galaxies are dwarfs ($M_B > -20$). Elsewhere, Haines et al. (2011) found an excess of blue dwarf galaxies ($M_r > -18$) around 1.5 Mpc from the centre of the Shapley supercluster, while Mahajan et al. (2010) discovered a similar incidence of excessive blue dwarfs on the outskirts of the Coma cluster ($z = 0.03$). In the Coma supercluster ($z = 0.03$), dwarf galaxies exhibit a stronger star formation–density relation than their massive counterparts (Mahajan et al. 2010). In an accompanying study of dwarf galaxies in the Coma supercluster, Mahajan et al. (2011a) showed that all the post-starburst k+A galaxies are dwarfs, and are found in or around the clusters and groups in the supercluster.

These results are in agreement with those presented by Smith et al. (2008), who showed that the red-sequence dwarf ($M_r \gtrsim -17.5$) galaxies on the outskirts of the Coma cluster have been truncated of star formation. Due to the flux limitations of the SDSS data used in this work, the low-luminosity ($M_r \geq -20.5$) galaxies could not be included in this analysis, but the picture portrayed above will hold for them too. The only exception in case of dwarf galaxies might be the absence of the second burst seen near ($\sim 0.5 r_{200}$) the cluster centre (Fig. 6). This is because amongst others, evaporation of cold gas becomes very important for dwarf galaxies (Fujita 2004; Boselli & Gavazzi 2006). Hence even a relatively softer encounter with a more massive galaxy may lead to the loss of all gas via tidal stripping and/or evaporation.

4.2 Star formation and the large-scale structure

In order to evaluate their role in the evolution of galaxies, it is crucial to understand the properties of galaxies on supercluster filaments. High-resolution simulations suggest that low overdensity regions like galaxy filaments can host a significant fraction of gas with temperatures between 10^5 and 10^7 K (Cen & Ostriker 1999; Croft et al. 2001; Phillips, Ostriker & Cen 2001; Dolag et al. 2006; Edwards et al. 2010b). This gas may be detected as radio emission (e.g. Kim et al. 1989), or through bremsstrahlung emission in soft X-rays (e.g. Dolag et al. 2006). But not only is the signal too weak for the present-day detectors, but the former can be employed only for very nearby cluster pairs. Hydrodynamical dark matter (+gas) simulations (e.g. Dolag et al. 2006) find that due to very low gas densities and low temperatures ($<10^7$ K), it is very difficult to observe these filaments directly. Recent *Suzaku* observations (Mitsuishi et al. 2012) seem to have confirmed (also Kull & Böhringer 1999, from ROSAT) an excess of hot X-ray gas in the filament joining the two rich Abell clusters in the core of the Shapley Supercluster. These observations are currently very difficult, and with no advanced X-ray observatory in the horizon, indirect ways of understanding the role of filaments in the evolution of cosmos, by studying the effect of the filamentary environment on the galaxies, are necessary (e.g. Porter & Raychaudhury 2007; Boué et al. 2008; Fadda et al. 2008; Porter et al. 2008).

By employing semi-analytic modelling, González & Padilla (2009) showed that galaxies with similar local density but different 'global' environment (i.e. different positions on the cosmic web) have subtle but non-negligible differences in their SFR and colours. They attribute this result to the coherent motion of galaxies approaching the clusters through large-scale filaments (Porter & Raychaudhury 2007; Fadda et al. 2008; Porter et al. 2008; Edwards et al. 2010a). Struck (2006) discussed an interesting scenario, whereby galaxies in a small galaxy group crossing a cluster may be pulled towards each other, thus increasing the local galaxy density by an order of magnitude, and the probability of galaxy–galaxy interactions by about a factor of 100 (density squared). Fig. 12 provides some evidence in support of this scenario (also see Gavazzi et al. 2003; Moss 2006; Oemler et al. 2009). For galaxies at $1 \leq r_{200} \leq 2$ from the cluster centre, the mean projected distance to the three nearest neighbours within $\pm 2,000$ km s^{-1} of the starburst galaxies is <1 Mpc in 78 per cent of the cases. However, for all other cluster galaxies in the same radial range, this is true only about 66 per cent of the time, suggesting that at a given cluster-centric distance, starburst galaxies are more likely to be in a relatively denser environment. This is worth verifying in larger samples as they become available.

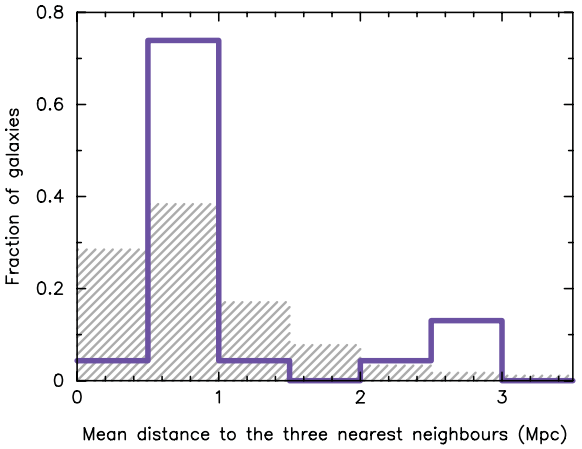

Figure 12. The mean distance to the three nearest neighbours, within a redshift slice of ± 2000 km s^{-1}, for galaxies 1–2 r_{200} from the cluster centre. The purple distribution shows the starburst galaxies, while the grey hatched histogram represents other cluster galaxies at the same radial distance from the cluster centre. We exclude galaxies which do not have at least three neighbours within this range.

Type I (straight) filaments exist between close ($\lesssim$5–10 Mpc) cluster pairs (Colberg et al. 2005; Dolag et al. 2006; PDH04). However, the majority ($\geq$50 per cent) of the filaments in the cosmic web are of type II (warped). Some attempts have also been made to understand the density profile of type I filaments (Colberg et al. 2005, also see Edwards et al. 2010b). Their relatively shorter length (Colberg et al. 2005; Dolag et al. 2006; PDH04) and higher matter density may imply that the probability of galaxy–galaxy interactions occurring amongst galaxies on these filaments is higher than on their counterparts. Fig. 8 favours this scenario. It shows that $\sim$32 per cent of the (morphologically classifiable) filaments feeding the comparison (CN) clusters are of type I (straight), as compared to $\sim$47 per cent in the SB clusters. This is also in sync with the results of Colberg et al. (2005), who showed that in the cold dark matter Universe, more massive structures are more strongly clustered than their less massive counterparts. Hence, the unrelaxed SB clusters ($\sigma_v \gtrsim 500$ km s^{-1}) are more likely to have a straight filament connecting them to a nearby companion cluster. We note that the detection of a significant fraction of our filaments remains uncertain because of low galaxy ($M_r \leq -20.5$) densities, so the quantities mentioned in this section may only be considered representative and not precise.

On a final note, we suggest that SB clusters are most likely dynamically unrelaxed clusters, presently being assembled via galaxies falling in through straight filaments. The occurrence of starburst galaxies on the periphery of these clusters is a direct consequence of the way local conditions (i.e. galaxy density and relative velocity) are affected by the global layout of the cosmic web.

4.3 Future implications

Compared to galaxies at $z \sim 0$, distant galaxies are more gas-rich. Hence it would not be an exaggeration to say that such events of spectacular starbursts would be more commonly seen at higher redshifts. Confirmation of this, however, can only result from the study of an unbiased sample of high-redshift clusters, observed up to their infall regions (e.g. Kartaltepe et al. 2008; Verdugo et al. 2008, also see Coppin et al. 2011 for recent observations of star formation related far-infrared emission on the outskirts of clusters at $z \sim 0.25$).

Once such data are available, one can ask whether the excess of star-forming galaxies observed in clusters at higher redshifts, the well-known 'Butcher–Oemler effect' (Butcher & Oemler 1984), is linked to the occurrence of starbursts in infalling galaxies, which appear to be nearer the cluster centre in projection (e.g. Oemler et al. 2009). For a sample of X-ray-luminous clusters at $0.18 < z < 0.55$, Ellingson et al. (2001) showed that the galaxy population in the cluster cores are the same at all epochs, but higher redshift clusters have a steeper gradient in the fraction of blue galaxies when the regions outside the core ($>0.5r_{500}$) are considered. Such colour-based studies, however, may have inherent problems due to the non-negligible fraction of galaxies that deviate from the normal correspondence between photometric colours and spectroscopically derived SFR (see Mahajan & Raychaudhury 2009, for instance). Another interesting idea to explore, though relatively more plausible in simulations, is finding the likelihood of detecting a starburst galaxy on a filament feeding a cluster along the LOS. Such a galaxy will appear near the centre of cluster, yet showing physical and intrinsic properties as that of its counterparts far away from the cluster core (see e.g. Oemler et al. 2009).

It would be very interesting to study the intermediate-mass/dwarf ($M_r > -20.5$) galaxies, in the infall regions of the SB clusters, which may be harassed even more easily by their relatively massive counterparts. One needs to perform a detailed morphological analysis of the starburst galaxies, such as those studied in this work. Considering galaxy–galaxy harassment to be the dominant environmental mechanism affecting the star formation properties of galaxies on cluster outskirts, one expects to see signatures of tidal interactions with neighbouring galaxies in visible or other short wavelength data (e.g. Smith et al. 2010). Unfortunately, the spatial resolution of the SDSS photometry, used in this work, is not suitable for this, which we leave for future follow-up.

5 SUMMARY AND CONCLUSIONS

Using the integrated SFR (and SFR/M^*) derived by B04 for galaxies in the SDSS DR4, the star formation properties of galaxies ($M_r \leq -20.5$) in the nearby ($0.02 \leq z \leq 0.15$) Abell clusters were analysed. The main results are summarized as follows.

(i) Star formation activity in galaxies on the outskirts of some clusters is enhanced near their periphery (r_{200}) and further into the clusters at $\sim 0.5r_{200}$. In agreement with several other observational and simulations' studies, we find that this enhancement in the SFR of galaxies on the clusters' periphery is most likely due to enhanced galaxy–galaxy interactions.

(ii) Starburst galaxies on cluster outskirts inhabit relatively denser environments, compared to other cluster galaxies at similar distances from the cluster centre.

(iii) Clusters with evidence of enhanced star formation activity on their periphery are likely to be dynamically unrelaxed, and fed by straight and well-defined supercluster filaments.

(iv) The infalling galaxies ($1.4 \leq r/r_{200} \leq 2.8$) in our clusters are a mix of galaxies that have passed through the cluster core at least once (the 'backsplash' population), and those which are falling into the cluster for the first time.

ACKNOWLEDGMENTS

Funding for the SDSS has been provided by the Alfred P. Sloan Foundation, the Participating Institutions, the National Aeronautics and Space Administration, the National Science Foundation, the U.S. Department of Energy, the Japanese Monbukagakusho and the Max Planck Society. The SDSS Web site is http://www.sdss.org/.

This research has made use of the X-Rays Clusters Database (BAX) which is operated by the Laboratoire d'Astrophysique de Tarbes-Toulouse (LATT), under contract with the Centre National d'Etudes Spatiales (CNES). Mahajan and Raychaudhury thank Professor Trevor J. Ponman and Professor Bianca Poggianti for their critique, which helped in improving the contents of this paper. We would like to thank the anonymous reviewer whose suggestions helped us in presenting this paper in a broader context. Mahajan was supported by grants from the ORSAS, UK, and the University of Birmingham.

REFERENCES

Abell G. O., Corwin H. G., Jr, Olowin R. P., 1989, ApJS, 70, 1
Abramson A., Kenney J. D. P., Crowl H. H., Chung A., van Gorkom J. H., Vollmer B., Schiminovich D., 2011, AJ, 141, 164
Adelman-McCarthy J. K. et al., 2006, AJS, 162, 38
Baldwin J. A., Phillips M. M., Terlevich R., 1981, PASP, 93, 5
Balogh M. L., Morris S. L., Yee H. K. C., Carlberg R. G., Ellingson E., 1999, ApJ, 527, 54
Balogh M. L., Navarro J. F., Morris S. L., 2000, ApJ, 540, 113
Balogh M. L. et al., 2004, MNRAS, 348, 1355
Beers T. C., Flynn K., Gebhardt K., 1990, ApJ, 100, 32
Bekki K., 1999, ApJ, 510, L15
Biviano A., Katgert P., Mazure A., Moles M., den Hartog R., Perea J., Focardi P., 1997, A&A, 321, 84
Biviano A., Fadda D., Durret F., Edwards L. O. V., Marleau F., 2011, A&A, 532, A77
Blanton M. R. et al., 2005, AJ, 129, 2562
Boselli A., Gavazzi G., 2006, PASP, 118, 517
Boué G., Durret F., Adami C., Mamon G. A., Ilbert O., Cayatte V., 2008, A&A, 489, 11
Braglia F., Pierini D., Böhringer H., 2007, A&A, 470, 425
Brinchmann J., Charlot S., White S. D. M., Tremonti C., Kauffmann G., Heckman T., Brinkmann J., 2004, MNRAS, 351, 1151 (B04)
Bruzual A. G., 1983, ApJ, 273, 105
Butcher H., Oemler A., Jr, 1984, ApJ, 285, 426
Carlberg R. G., Yee H. K. C., Ellingson E., 1997, ApJ, 478, 462
Cen R., Ostriker J. P., 1999, ApJ, 514, 1
Colberg J. M. et al., 2000, MNRAS, 319, 209
Colberg J. M., Krughoff K. S., Connolly A. J., 2005, MNRAS, 359, 272
Coppin K. E. K. et al., 2011, MNRAS, 416, 680
Cortese L. et al., 2007, MNRAS, 376, 157
Croft R. A. C., Di Matteo T., Davè R., Hernquist L., Katz N., Fardal M. A., Weinberg D. H., 2001, ApJ, 557, 67
De Lucia G., Blaizot J., 2007, MNRAS, 375, 2
De Propris R. et al., 2004, MNRAS, 351, 125
Diaferio A., Geller M. J., 1997, ApJ, 481, 633
Dolag K., Meneghetti M., Moscardini L., Rasia E., Bonaldi A., 2006, MNRAS, 370, 656
Edwards L. O. V., Fadda D., Frayer D. T., 2010a, ApJ, 724, L143
Edwards L. O. V., Fadda D., Frayer D. T., Lima Neto G. B., Durret F., 2010b, AJ, 140, 1891
Ellingson E., Lin H., Yee H. K. C., Carlberg R. G., 2001, ApJ, 547, 609
Fadda D., Biviano A., Durret F., 2008, ApJ, 672, L9
Feulner G., Goranova Y., Drory N., Hopp U., 2005, MNRAS, 358, L1
Fujita Y., 1998, ApJ, 509, 587
Fujita Y., 2004, PASJ, 56, 29
Gavazzi G., Cortese L., Boselli A., Iglesias-Paramo J., Vìlchez J. M., Carrasco L., 2003, ApJ, 597, 210
Gavazzi G., Fumagalli M., Cucciati O., Boselli A., 2010, A&A, 517, A73
Gill S. P. D., Knebe A., Gibson B. K., 2005, MNRAS, 356, 1327
Gnedin O. Y., 2003, ApJ, 582, 141
Gómez P. L. et al., 2003, ApJ, 584, 210

González R. E., Padilla N. D., 2009, MNRAS, 397, 1498
Haines C. P., La Barbera F., Mercurio A., Merluzzi P., Busarello G., 2006, ApJ, 647, L21
Haines C. P., Gargiulo A., La Barbera F., Mercurio A., Merluzzi P., Busarello G., 2007, MNRAS, 381, 7
Haines C. P., Busarello G., Merluzzi P., Smith R. J., Raychaudhury S., Mercurio A., Smith G. P., 2011, MNRAS, 412, 127
Kapferer W., Sluka C., Schindler S., Ferrari C., Ziegler B., 2009, A&A, 499, 87
Kartaltepe J. S., Ebeling H., Ma C. J., Donovan D., 2008, MNRAS, 389, 1240
Kauffmann G. et al., 2003, MNRAS, 341, 33
Kauffmann G., White S. D. M., Heckman T. M., Menàrd B., Brinchmann J., Charlot S., Tremonti C., Brinkmann J., 2004, MNRAS, 353, 713
Keel W. C., 2005, AJ, 129, 1863
Kim K.-T., Kronberg P. P., Giovannini G., Venturi T., 1989, Nat, 341, 720
Kraft R. P. et al., 2011, ApJ, 727, 41
Kull A., Böhringer H., 1999, A&A, 341, 23
Lake G., Katz N., Moore B., 1998, ApJ, 495, 152
Lee H., Richer M. G., McCall M. L., 2000, ApJ, 530, L17
Lewis I. et al., 2002, MNRAS, 334, 673
Maaike D., Labbè I., Franx M., van Dokkum P. G., Taylor E. N., Gawiser E. J., 2009, ApJ, 690, 937
Madgwick D. S. et al. (the 2dFGRS team), 2002, MNRAS, 333, 133
Mahajan S., Raychaudhury S., 2009, MNRAS, 400, 687
Mahajan S., Haines C. P., Raychaudhury S., 2010, MNRAS, 404, 1745
Mahajan S., Haines C. P., Raychaudhury S., 2011a, MNRAS, 412, 1098
Mahajan S., Mamon G. A., Raychaudhury S., 2011b, MNRAS, 416, 2882
Mamon G. A., Sanchis T., Salvador-Solè E., Solanes J. M., 2004, A&A, 414, 445
Marcillac D., Rigby J. R., Rieke G. H., Kelly D. M., 2007, ApJ, 654, 825
Mayer L., Mastropietro C., Wadsley J., Stadel J., Moore B., 2006, MNRAS, 369, 1021
Mercurio A., Busarello G., Merluzzi P., Barbera F. La, Giradi M., Haines C. P., 2004, A&A, 424, 79
Mitsuishi I. et al., 2012, PASJ, 64, 18
Moore B., Katz N., Lake G., Quinn, Dressler A., Oemler A., Jr, 1996, Nat, 379, 613
Moran S. M., Ellis R. S., Treu T., Smail I., Dressler A., Coil A. L., Smith G. P., 2005, ApJ, 634, 977
Moss C., 2006, MNRAS, 373, 167
Noeske K. G. et al., 2007, MNRAS, ApJ, 660, L47
Oemler A., Dressler A., Kelson D., Rigby J., Poggianti B. M., Fritz J., Morrison G., Smail I., 2009, ApJ, 693, 152
Phillips L. A., Ostriker J. P., Cen R., 2001, ApJ, 554, L9
Pimbblet K. A., Drinkwater M. J., Hawkrigg M. C., 2004, MNRAS, 354, L61 (PDH04)
Pimbblet K. A., Smail A., Edge A. C., O'Hely E., Couch W. J., Zabludoff A. I., 2006, MNRAS, 366, 645
Pivato M. C., Padilla N. D., Lambas D. G., 2006, MNRAS, 373, 1409
Poggianti B. M., Smail I., Dressler A., Couch W. J., Barger A. J., Butcher H., Ellis R. S., Oemler A., Jr, 1999, ApJ, 518, 576
Poggianti B. M. et al., 2006, ApJ, 642, 188
Popescu C. C. et al., 2005, ApJ, 619, L75
Popesso P., Biviano A., Bohringer H., Romaniello M., 2007, A&A, 461, 397
Porter S. C., Raychaudhury S., 2007, MNRAS, 375, 1409
Porter S. C., Raychaudhury S., Pimbblet K. A., Drinkwater M. J., 2008, MNRAS, 388, 1152
Prescott M. K. M. et al., 2007, ApJ, 668, 182
Reverte D., Vìlchez J. M., Hernàndez-Fernàndez J. D., Iglesias-Pàramo J., 2007, AJ, 133, 705
Rines K., Geller M. J., Kurtz M. J., Diaferio A., 2005, AJ, 130, 1482
Sato T., Martin C. L., 2006, ApJ, 647, 946
Schirmer M., Suyu S., Schrabback T., Hildebrandt H., Erben T., Halkola A., 2010, A&A, 514, A6
Smith R. J. et al., 2008, MNRAS, 386, L96
Smith R. J. et al., 2010, MNRAS, 408, 1417
Sol Alonso M., Lambas D. G., Tissera P., Coldwell G., 2006, MNRAS, 367, 1038
Struble M. F., Rood H. J., 1999, ApJS, 125, 35
Struck C., 2006, in Mason J. W., ed., Astrophysics Update 2. Springer, Heidelberg, p. 115
Sun M., Murray S. S., 2002, AJ, 577, 139
Sun M., Donahue M., Roediger E., Nulsen P. E. J., Voit G. M., Sarazin C., Forman W., Jones C., 2010, ApJ, 708, 946
Tonnesen S., Bryan G. L., 2010, ApJ, 709, 1203
Verdugo M., Ziegler B. L., Gerken B., 2008, A&A, 486, 9
Verdugo M., Lerchster M., Böhringer H., Hildebrandt H., Ziegler B. L., Erben T., Finoguenov A., Chon G., 2012, MNRAS, 421, 1949
Wang Q. D., Owen F., Ledlow M., 2004, ApJ, 611, 821
Wolf C. et al., 2009, MNRAS, 393, 1302
Yamagami T., Fujita Y., 2011, PASJ, 63, 1165
Yang X., Mo H. J., Van den Bosch F. C., Pasquali A., Li C., Barden M., 2007, ApJ, 671, 153
Zel'dovich I. B., Einasto J., Shandarin S. F., 1982, Nat, 300, 407

This paper has been typeset from a TEX/LATEX file prepared by the author.